

## Computation of Flow around a Rotating Flying Disk

Yumi Yamashita<sup>†</sup>, Tetuya Kawamura<sup>†</sup>

Graduate School of Integrated Sciences, Ochanomizu University<sup>†</sup>

(Received June 14, 2007)

### Abstract

The flow around a rotating disk placed in a uniform stream is simulated numerically by solving the incompressible Navier-Stokes equations. The overlaid grid system, the pair of a cylindrical grid and a vertical grid, has been implemented to compute the flow around the whole disk. Third order upwind scheme is employed since it has produced reasonable results also in turbulent high Reynolds number flows. The nature of the boundary layer formation on the moving disk surface is investigated, and the effects of the advance ratio, angle of attack and Reynolds number on the flow fields are examined and compared with experiments.

Key Words: Flying disk, Overlaid grid system, Third order upwind scheme

### 1. Introduction

Various physical phenomena on high Reynolds flow around various wing plan forms have been elucidated with experimental analyses and numerical simulations in the past. A disk flying at a moderate angle of attack may be regarded as a conventional wing with a small aspect ratio. Circular planforms have been applied to airplanes like the XF5U in the past, and as a more recent example, in "Micro Air Vehicles".

Other applications of a flying disk are related to sports aerodynamics and are accompanied by spin stabilization. Circular planforms have been applied to airplanes like the XF5U in the past, and as a more recent example, in "Micro Air Vehicles". Other applications of a flying disk are related to sports aerodynamics and are accompanied by spin stabilization.

Several experimental reports on the flow around a flying disk have been published recently. Higuchi et al.<sup>1</sup> reported an experimental investigation on the flow past a flying disk in low-speed wind tunnel, and detailed flow characteristics within the boundary layer as well as in the vortex wake have been cleared. Potts et al.<sup>2</sup> have reported in one of their recent papers a type of surface vortex generators to control aerodynamic moment. The present work compliments the experimental studies and addresses the fluid dynamical phenomena around a flying disk with numerical simulations. In particular, numerical results are compared with the results of experiment by Higuchi et al.<sup>1</sup>.

The behavior of the boundary layer over a moving wall with or without separation layer<sup>3</sup> is also of a fundamental interest. The flight trajectories of a disk can be simulated by using parameters obtained from this simulation of the flow around a flying disk.

## 2. Numerical Schemes

The flow around a flying disk was simulated by solving the 3-dimensional incompressible Navier-Stokes equations. Standard MAC method was used as an algorithm to solve the governing equations. The Poisson equation for pressure term that appears in a stage of Standard MAC method was solved with SOR (Successive Over-Relaxation) method. Euler's explicit method of first order accuracy was used as a time differential scheme. The 3<sup>rd</sup> order upwind differential scheme (Eqn.1) is used for convection term. This approximation uses 5 points arranged around the target point.

$$\begin{aligned}
 f\left(\frac{du}{dx}\right)_{x=x_i} &= \frac{f(2u_{i+1} + 3u_i - 6u_{i-1} + u_{i-2})}{6\Delta x} & (f \geq 0) \\
 &= \frac{f(-u_{i+2} + 6u_{i+1} - 3u_i - 2u_{i-1})}{6\Delta x} & (f < 0)
 \end{aligned}
 \tag{1}$$

where  $u$  is the velocity in the uniform flow direction,  $x$ , and identification  $i$  shows  $x$ -directional position for referenced points. 2<sup>nd</sup> order central differential scheme is used for the other spatial terms. Implicit LES (Large Eddy Simulation) method<sup>4</sup> is adopted as a turbulence model after comparison with results of LES (Large Eddy Simulation) method.

The differentials of Navier-Stokes equations are normalized with 3-dimensional coordinate transformation method.

## 3. Spatial Models

The 3-dimensional overlaid grid system where two grids are partly overlaid each other, is used in this study to properly fit the grids on the surface of a flying disk. The cylindrical grid that can fit circumference of a flying disk is adopted as the grid for periphery space. This cylindrical grid has the singularity at the center of the grid, and this condition makes it impossible to solve the differentials of Navier-Stokes equations at that singularity. To resolve this problem, the Cartesian grid is adopted at the center of the cylindrical grid and partly overlaid with the cylindrical grid as shown in Fig 1.

The simulation for the entire domain is realized by interpolating values between the partly overlaid grids.

The communication between these two grids is achieved by setting values at the boundary points and interpolating from values at the surrounding points on the other grid. The 3-dimensional "in-out decision method" is used to determine the surrounding points. The parametric elements method (Eqn.2) is used to determine the interpolation factors for values at surrounding points.

$$\begin{aligned}
f(x) &= N_1 \cdot x_1 + N_2 \cdot x_2 + N_3 \cdot x_3 + N_4 \cdot x_4 + N_5 \cdot x_5 + N_6 \cdot x_6 + N_7 \cdot x_7 + N_8 \cdot x_8 \\
N_1 &= (1-\xi)(1-\eta)(1-\zeta) \\
N_2 &= \xi(1-\eta)(1-\zeta) \\
N_3 &= \xi\eta(1-\zeta) \\
N_4 &= (1-\xi)\eta(1-\zeta) \\
N_5 &= (1-\xi)(1-\eta)\zeta \\
N_6 &= \xi(1-\eta)\zeta \\
N_7 &= \xi\eta\zeta \\
N_8 &= (1-\xi)\eta\zeta
\end{aligned} \tag{2}$$

Eqn.2 gives a function for x-coordinate, and functions for y and z coordinates can be similarly obtained as well. Three unknowns ( $\xi$ ,  $\eta$  and  $\zeta$ ) are solved with those three functions. Then interpolation factors,  $N_1$  to  $N_8$ , can be determined explicitly. The values at the boundaries are determined by summing the values at the 8 surrounding points multiplied by the individual interpolation factor. The communication between grids can be realized by interpolating values at the boundaries with these techniques.

#### 4. Settings for Simulation

The model of a flying disk for this simulation is "Eagle" which is commercially available from Innova Champion Disks Inc. It is designed for disk golf game. The cross-sectional view is shown in Fig.2. The Reynolds number is chosen as  $Re=1.1 \times 10^5$ . This corresponds to 8m/s of flow velocity in air. These settings coincide with the experiment by Higuchi et al<sup>1</sup>.

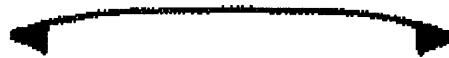


Fig.2: "Eagle" of Innova Inc.

The central region of grids is shaped to fit the form of a flying disk as shown in Fig.3. Since this is not the boundary-fitted coordinate, the region for an obstacle is manipulated by masking.

Slip condition is set for vertical boundary, uniform flow is set for outer boundary, and non-slip condition is imposed on the solid surface. In this simulation, the rotating velocity of a flying disk is imposed as the boundary condition of velocity around the object. The angle of attack is implemented as the incoming angle of uniform flow.

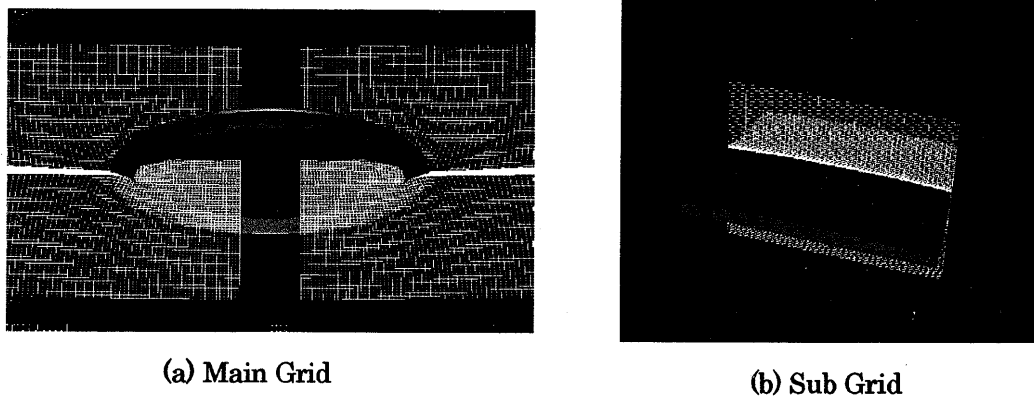


Fig.3: overlaid grid system for "Eagle"

## 5. Results

Simulations of flow around a flying disk on several cases of settings were simulated. Two parameters, the angle of attack and rotational speed, were varied to study their effects on the flow.

### 5.1 Velocity Profiles

The differences between the cases of angles of attack 0 and 5 degrees can be seen in Figs.4. The figures show cross sections at  $y/D$  (span-wise direction normalized by diameter)= 0.5. The color code correspond to high speed in red and low to negative velocity in blue (numerical values to be included in the final figures.) Reverse flow region on the upper surface at 5 degrees is evident in Fig.4 (b). Although Fig.4 (a) also has blue region on the upper surface, this region still have positive values. On the other hand, the large recirculation region on the lower surface behind a backward-facing region (grip) is prominent at 0 degree.

The characteristic crescent form of reattachment is distorted when viewed from the top (to be shown in the full paper) with disk rotation.

### 5.2 Wall Shear Stress

Figures 5 shows the calculated wall shear stress distribution on the upper surface at angle of attack of 5 degrees.

With zero rotation flow separation occurs at the leading edge and the curved reattachment line is observed (Fig.5 (a)). The shear stress grows monotonically toward the trailing edge. The wall shear stress distribution was consistent with the velocity profiles.

The effect of the disk rotation can be seen in Fig.5 (b). The rotation is in the clockwise direction. The leading edge separation region is swept back, whereas the

advancing wall movement generates high-shear stress region.

### Summary

Flow around a flying disk has been numerically simulated using an implicit LES method. A three-dimensional Overlaid Grid System has been implemented to alleviate the center singularity and to improve the resolution. It was confirmed that this grid system could calculate properly even at the center of the disk. Flow phenomena around a flying disk including flow separation and transition have been investigated. The results generally agreed with the experiment, and the results will be presented and discussed in detail in the full paper.

### References

1. Higuchi, H., Goto, Y., Hiramoto, R. & Meisel, I., "Rotating Flying Disks and Formation of Trailing Cortices", AIAA 2000-4001, 18th AIAA Applied Aero. Conf., Denver, CO, Aug. 2000.
2. Potts, J.R. & Crowther, W.J., "Flight Control of a Spin Stabilised Axi-symmetric Disc-wing", AIAA 2001-0253, 39th Aero. Sci. Meet & Exhibit, Reno, NV, USA, Jan. 2001.
3. Sears, W.R. and Telionis, D.P., "Unsteady Boundary-Layer Separation," Proceedings of SQUID Workshop, June 1971, Purdue University.
4. Komurasaki, S. & Kuwahara, K., "Implicit Large Eddy Simulation of a Subsonic Flow Around NACA0012 Airfoil", AIAA 2004-594, 42<sup>nd</sup> Aero Sci. Meet & Exhibit, Reno NV, USA, Jan. 2004.

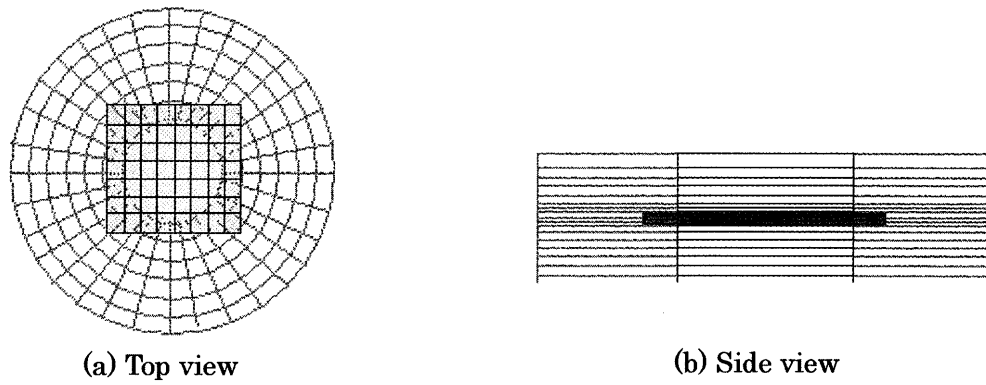


Fig.1: 3-dimensional overlaid grid system

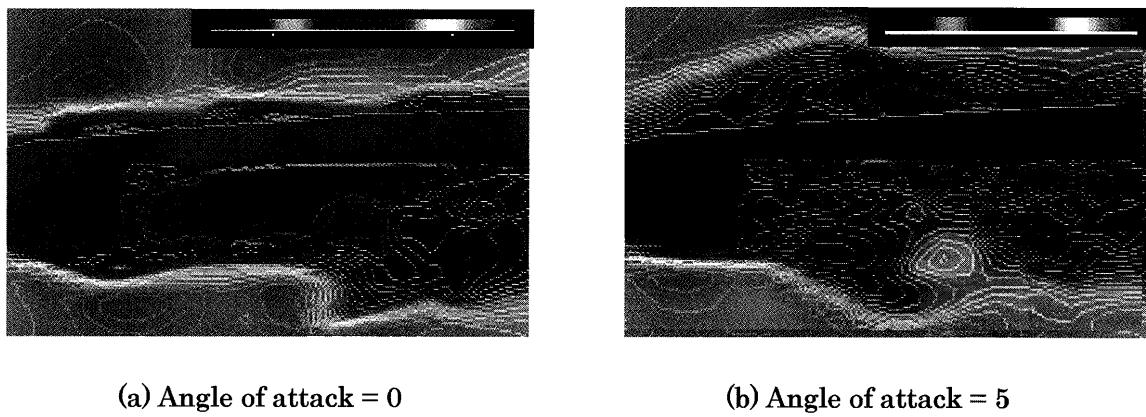


Fig.4: Instantaneous Velocity at the  $y/D=0.5$  (advancing ratio=0.0)

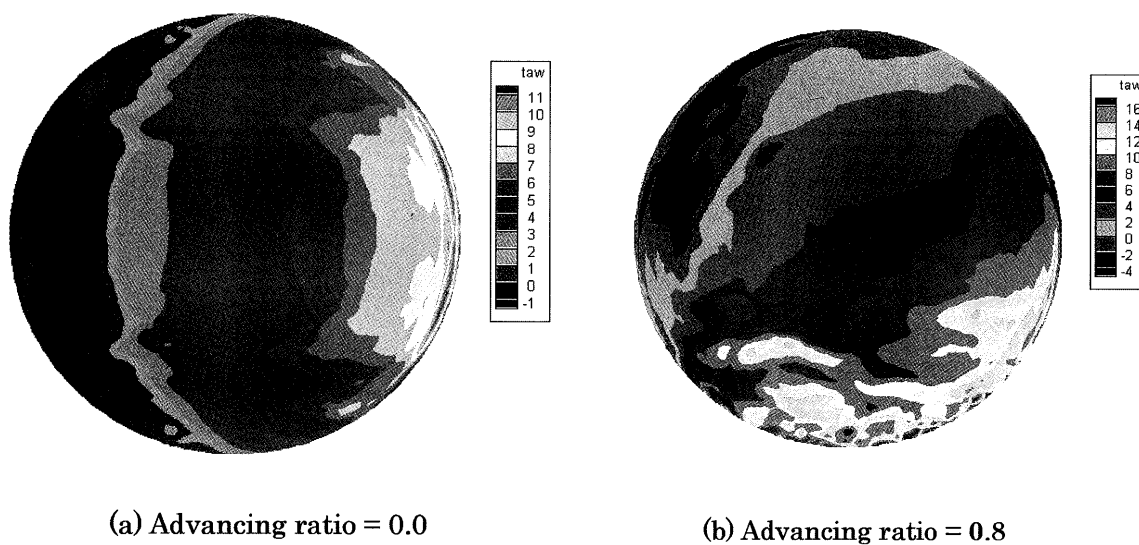


Fig.5 Wall Shear Stress on uppersurface (angles of attack=5)